Asociación Argentina
de Mecánica Computacional

Mecánica Computacional Vol XXVII, págs. 2541-2554 (artículo completo)
Alberto Cardona, Mario Storti, Carlos Zuppa. (Eds.)
San Luis, Argentina, 10-13 Noviembre 2008

GENETIC ALGORITHMS AND FM-BEM FOR THE MICROSTRUCTURE OPTIMIZATION OF MICRO-HETEROGENEOUS MATERIALS WITH FUNCTIONAL-GRADED THERMAL CONDUCTIVITY

Marco Dondero, Adrián P. Cisilino

División Soldadura y Fractomecánica, INTEMA (CONICET), Facultad de Ingeniería, Universidad Nacional de Mar del Plata, JB Justo 4302, 7600 Mar del Plata, Argentina, mdondero@fi.mdp.edu.ar, cisilino@fi.mdp.edu.ar

Keywords: Genetic Algorithms, Fast Multipole Boundary Element Method, Microstructure Optimization, Functionally Graded Materials.

Abstract. A numerical tool for the design of micro-heterogeneous materials with customized heat conduction properties is presented in this paper. The spatial variation of the local material properties is achieved via the optimization of the spatial distribution of the holes/inclusions. A Genetic Algorithm (GA) is used for this purpose. Although very effective and versatile GAs are computationally expensive. This problem is tackled in two ways here: a Fast Multipole Boundary Element Method algorithm is used for the thermal analysis of the microstructures, and the GA is implemented in parallel using a cluster of PCs. Two examples illustrate the performance of the developed implementation.

1 INTRODUCTION

Functionally graded materials (FGM) are two-component composites with a compositional gradient from the one component to the other in order to obtain a given spatial variation of the local material properties. FGM are very promising in applications where the operating conditions are severe. For example, wear-resistant linings, rocket heat shields, heat exchanger tubes, heat-engine components, plasma facings for fusion reactors, and electrical insulating metal/ceramic joints. The FGM concept originated in Japan in 1984 during the space plane project, in the form of a thermal barrier material capable of withstanding a surface temperature of 2000 K and a temperature gradient of 1000 ºK within a section equal to 10 mm. Since then, FGM thin films have been comprehensively researched and they are almost a commercial reality (Ruys et al. 2001).

The design of micro-heterogeneous materials with customized heat conduction properties is proposed and tested in this work. The material microstructure consists in continuous matrix with inclusions idealized as perfect insulated circular holes. The spatial distribution of the inclusions can be adjusted to obtain customized heat conduction properties.

One of the difficulties usually encountered in the computational design of random micro-heterogeneous materials is that the solution space is non-convex and the objective functions are not continuously differentiable. A numerical approach to simulate and accelerate the associated design process is due to Zhodi (2005) who proposed the utilization of Genetic Algorithms (GA).

Following Zhodi (2005), a high-performance numerical tool for the design of micro-heterogeneous materials with customized heat conduction properties is presented. Computations are carried on representative volume elements (RVE) which size is determined after a homogenization analysis. A GA is used as the optimization method, with the spatial distribution of the holes (inclusions) as design variables and the temperature profile along the sample as objective function. The GA is implemented in parallel using a PC cluster and the samples are solved using a Fast Multipole Boundary Element Method.

2 THE FAST MULTIPOLE BOUNDARY ELEMENT METHOD AND MODELING CONSIDERATIONS

Genetic Algorithms are robust global optimizers but they exhibit high computational cost resulting from the repetitive evaluation of the fitness function. As it will be seen in the following sections, the evaluation of the fitness function for this work requires the solution of thermal fields for computationally expensive RVE models containing a considerable number of inclusions. The Boundary Element Method (BEM) was selected for the solution of the thermal problem due to simplicity in the generation of the required data (the model discretization is restricted only to the boundaries) and the accuracy of the method (Aliabadi 2002).

The Fast Multipole Boundary Element Method (FMBEM) is used to reduce the computational cost in terms of both, operations and memory requirements of the direct BEM formulations. FMBEM reduces the computational cost of the direct BEM, from an order of $O(N^3)$ to a quasi-linear. This reduction is achieved by multilevel clustering of the boundary elements into cells, the use of the multipole series expansion for the evaluation of the fundamental solution in the far field and the use of an efficient iterative solver. The FMBEM used in this work is based on the work by Liu and Nishimura (2006). It uses a constant element discretization, analytical integration of the kernels and a preconditioned GMRES solver.

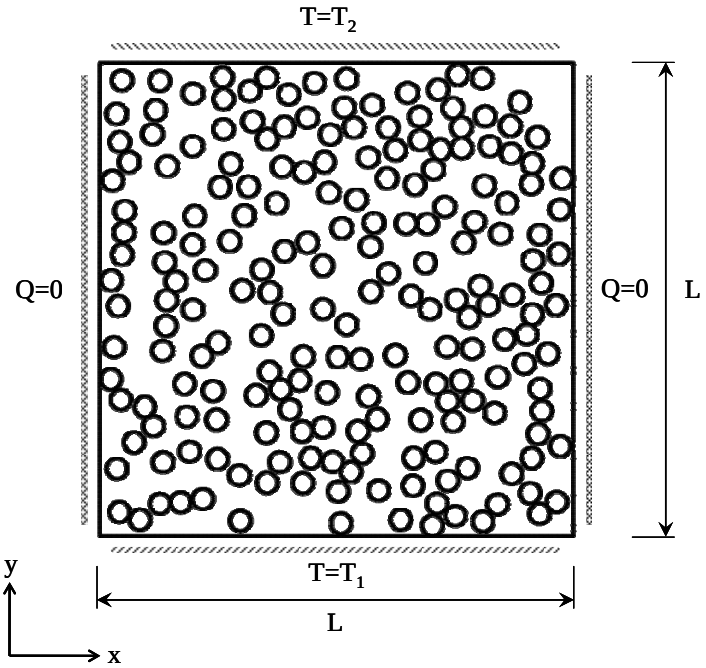

Figure 1: Representative volume element with a void fraction f= 0.3.

A typical model for the present application is illustrated in Figure 1. It consists in a two-dimensional idealization of the foam microstructure with the gas cells assimilated to isolated circular holes. Boundary conditions are specified in order to induce a one-dimensional heat flux in the y-direction. The model discretization strategy was devised after a convergence analysis. With this purpose a reference solution was computed using direct BEM for a problem similar to that of Figure 1, but containing 100 holes of radius r=L/31 (L being the specimen dimension) arranged on a regular square-array resulting in a void volume fraction (the ratio of the hole volume to the total sample volume) f=0.327. The independency of the BEM solution with respect to the size of the element was explored by means of the total potential energy U. The number of elements for the model was progressively increased and the results compared. Obtained results are illustrated in Figure 2 (dark symbols), where the potential energy values are normalized with respect to the total potential energy of a homogeneous hole-free specimen, U_0. From this analysis it was concluded that a model discretization with 4400 elements (40 elements per hole perimeter, 100 element along the sample side) provides mesh-independent results.

Afterwards, the FMBEM algorithm was "tuned-up" for optimum performance and accuracy for the problem under analysis. In this process it was necessary to adjust the elements-per-cell parameter which determines the extent of the near and far fields for the collocation points (Liu and Nishimura 2006). This parameter affects the quality of the solution and the efficiency of the algorithm. Figure 3 illustrates the deviation of the FMBEM results and the algorithm speed up with respect to the direct BEM as a function of the elements-per-cell parameter. Error computations were done by comparing the solutions for the two models on an element-by-element basis and the results are presented in terms of the mean error value and its standard deviation (error bars in the figure). Results in Figure 3 show that for values greater than 10 elements per cell, the relative error reduces noticeably and its dispersion vanishes. Similarly, the CPU time decreases for higher number of elements per cell, but it rapidly increases when this number is greater than 200. This change in the

tendency occurs when the size of the near field is too big and thus the algorithm ends up working like a direct BEM (one may imagine, as the extreme case, a picture consisting in a single cell enclosing the complete model in the near field). The convergence of the FMBEM and BEM solutions is also plotted in Figure 2. Figure 4 depicts the speed up of the algorithm as a function of the number of elements. Based on the above results the number of elements per cell was selected equal to 200 for further computations.

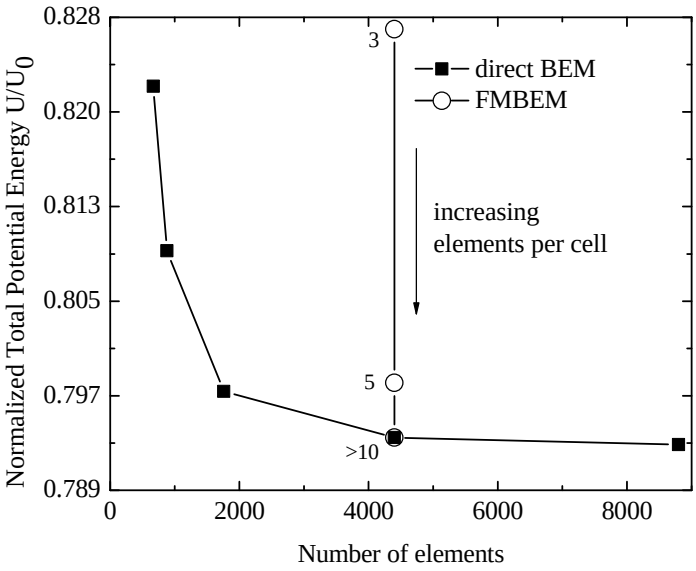

Figure 2: Normalized Total Potential Energy as a function of the number of elements.

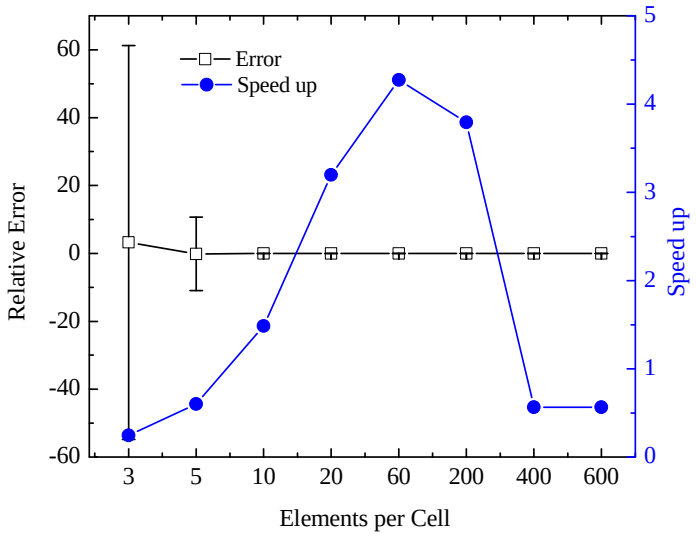

Figure 3: Relative error and FMBEM speed up vs. elements per cell for a 4400 element mesh.

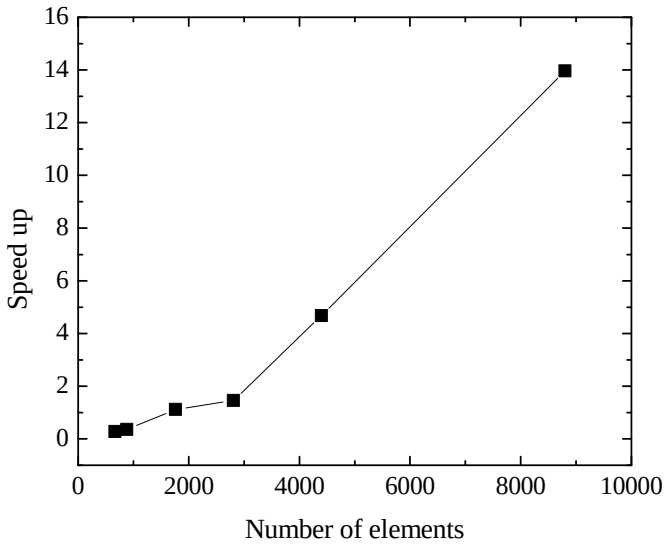

Figure 4: FMBEM speed up as a function of the number of elements.

3 THE REPRESENTATIVE VOLUME ELEMENT

The representative volume element (RVE) is the smallest sample of material which exhibits an invariant macroscopic response. This means that the sample must be big enough to hold a representative number of heterogeneities.

The micro heterogeneous material studied has a hole-matrix microstructure which is assumed to be two dimensional in this work. In addition, the holes are considered circular and randomly distributed. In order to size the RVE, a series of FMBEM analysis were performed for samples containing an increasing number of randomly distributed holes and the total potential energy has been computed in each case. In every case the model boundary conditions are that illustrated in Figure 1. The following hole per sample sequence was used to study the dependence of the effective responses on the sample size: 10, 30, 60, 100, 150, 200 and 300. In order to get more reliable response data, tests were performed 20 times for each hole number set (each time with a different hole distribution) and the results have been averaged. Three constant void fractions were studied f= 0.1, 0.3 and 0.45. Results for the case f=0.3 are illustrated in Figure 5. Similar results were obtained for f=0.1 and 0.45. Justified by the somewhat ad-hoc fact that for two successive enlargements of the number of holes the responses differed from one another, on average, by less than 0.5%, the 200-hole (inclusion) samples were selected as RVE for further tests.

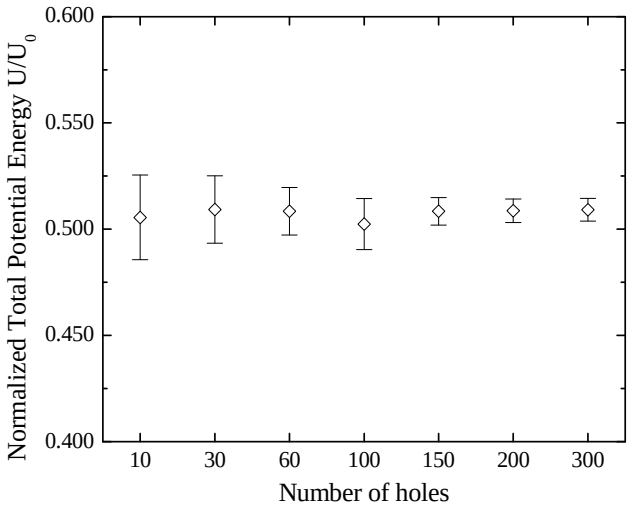

Figure 5: Potential energy as a function of the number of holes for f=0.3 void fraction. Error bars indicate result dispersion.

RVEs were used to compute the sample conductivity in terms of the void volume fraction, $k(f)$. This result will be used later in the examples section. Figure 6 illustrates the overall normalized conductivity k/k_0 for a series or RVE with void volume fractions in the range $0 \leq f \leq 0.5$ computed as $k(f)/k_0 = q \cdot L/(\Delta T \cdot k_0)$, k_0 being the conductivity of the matrix material and q the total one-dimensional flux in the y-direction. Each of the pints in the plot is the mean value of 4 computations. The error bars indicate the dispersion of the results, which are below 1% in every case. The results were fitted using a polynomial approximation as follows:

$$k(f)/k_0 = 1.0514 \cdot f^2 - 1.9553 \cdot f + 1 \qquad (1)$$

which has correlation coefficient R^2=0.9997.

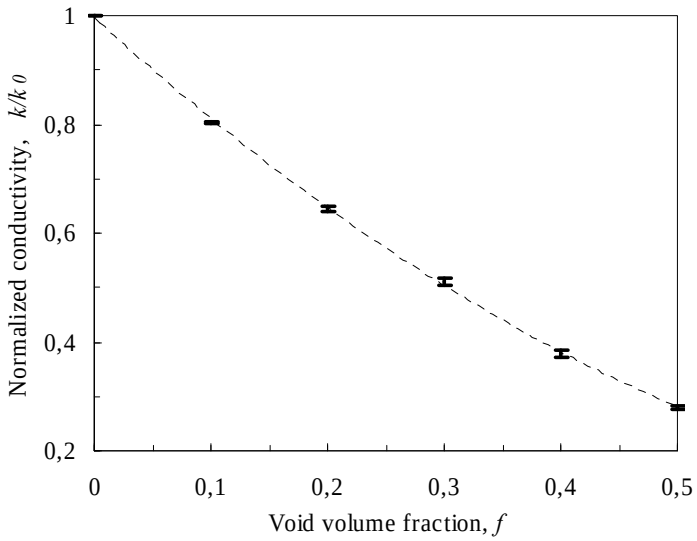

Figure 6: Normalized thermal conductivity as a function of the void volume fraction.

4 GENETIC ALGORITHMS

Genetic Algorithms (hereafter "GA") simulate the natural evolution; hence their components are the chromosomes, the genetic material that dictates unique properties of the individuals (Goldberg 1999). A GA emulates the phenomena that take place during reproduction of species making use of the genetic operators. The latest are natural selection, pairing and mutation. Individuals live in an environment determined by the objective (or fitness) function, where they compete for survival and only the best succeed. The GA code usied in this work is based on PIKAIA, a self-contained, genetic-algorithm-based optimization subroutine developed by Charbonneau and Knapp, and available in public domain in the internet (Charbonneau and Knapp 1995).

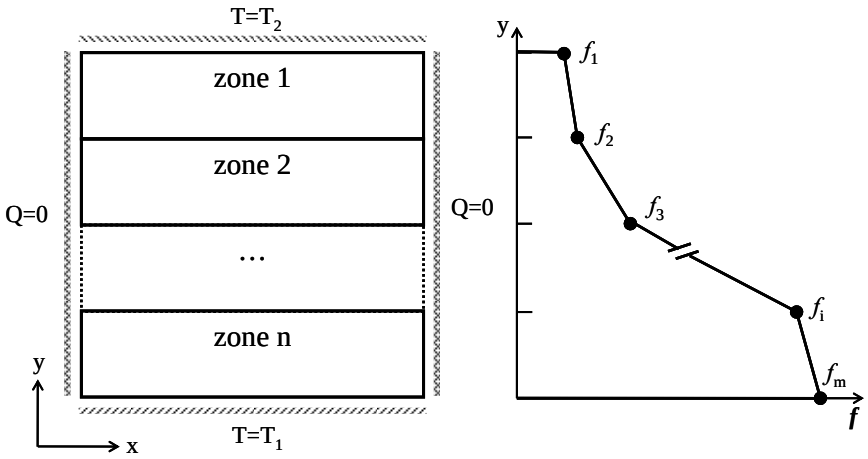

Figure 7: Domain division, boundary conditions and piecewise linear void fraction distribution of the RVE sample.

The GA is used to optimize the spatial distribution of the inclusions (holes) in the foam microstructure in order to obtain a given temperature distribution in the *y*-direction, *T(y)* (the objective function). The optimization problem is solved by dividing the model domain into *n* zones (parallel bands in Figure 7) of equal length with linear distribution of the void volume fraction. This approach results in a piecewise linear interpolation of the void volume fraction, *f*(*y*), which is defined in terms of *m=n+1* discrete f_i values. The f_i are selected as design variables for the GA and they are codified into a chromosome

$$chromosome = [f1, f2, \ldots, fm]. \tag{2}$$

The chromosome representation is done in binary format.

The fitness of the individuals (the fitness function) is the deviation of its temperature field from the objective temperature field, *T(y)*. This is assessed using a least-squares scheme for the differences between the FMBEM results and *T(y)* for a set of *p* internal points evenly distributed over the complete model domain:

$$fitness\ (individual\ i) = \frac{\sqrt{\sum_{j=1}^{p}\left[T(y_j)-t_j\right]^2}}{p} \tag{3}$$

where t_j is the temperature solution at the j^{th} internal point. In order to make the fitness value independent of the number of evaluation points the definition of the fitness function implies an average. The number of evaluations points can not be guaranteed constant for every model

due to the constant change in the void volume fraction during the optimization process and the random nature of the foam microstructure.

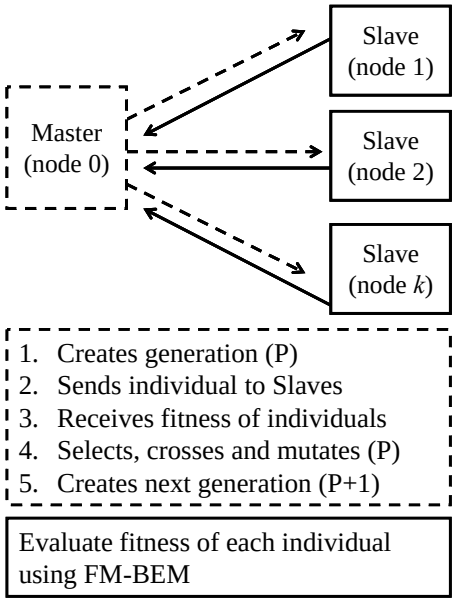

Figure 8: PAGA master/slave parallel implementation: master (broken lines) and slave (continuous lines) tasks and communication scheme (messages through MPI).

In every case the fitness function evaluation is performed using a model with dimensions greater than that of the RVE (see Section 2). The random distribution for the hole positions are generated automatically by using the rejection method with the piece-wise definition for *f(y)* as distribution function (Press et al. 1992).

The critical issue in the implementation of a GA is the computational cost of the evaluation of the fitness function, which must be performed hundreds or even thousands of times for the solution of a single problem. In order to accelerate the computations a parallel version of the GA was developed. The GA are relatively easy to implement in parallel due to natural independence in the evaluation of the fitness function for each individual. The developed algorithm uses a master-slave scheme where the master node is in charge of the management of the GA (creating and populating each generation) and the slave nodes are dedicated to the evaluation of the fitness of the individuals by solving the FMBEM models (see Figure 8). This was implemented by incorporating MPI routines to PIKAIA. The parallel version of the GA runs on a Beowulf cluster of 8 PC with GNU/Linux.

5 EXAMPLES

There are presented in this section two benchmark examples used for the validation of the proposed implementation. In both cases the objective function are temperature distributions, *T(y)*, corresponding to given thermal conductivities, *k(y)*. All computations are performed using a RVE with dimensions $L \times L$ = 60 mm ×60 mm with hole radios r= 1 mm and matrix thermal conductivity k_0= 1 W/mm·°C.

5.1 Piece-wise temperature distribution

The first example consists in a sample with the piece-wise linear objective temperature field (see Figure 9)

$$T(y) = 4.2 \cdot y - 62 \quad 0mm \le y \le 30mm,$$
$$T(y) = 1.2 \cdot y + 28 \quad 30mm < y \le 60mm. \qquad (4)$$

Boundary conditions are T_2=100°C along the side y=60mm and prescribed flux q = -1.25 W/mm^2 along the side y=0 mm. The lateral sides are insulated (see Figure 1).

It is easy to see that the above objective function is the temperature-field solution for the problem consisting in a two-zone sample with normalized thermal conductivities $[k(f)/k_0]_1 = 1$ and $[k(f)/k_0]_2 = 0.2852$. Note that the thermal conductivities for the zones are the limit values of equation 1, which correspond to void volume fractions f=0 and f=0.5 respectively.

The optimization domain is divided into 8 zones, resulting in nine design variables f_i. The chromosome was codified using 6 significant digits (i.e. the number of genes) per design variable. Parameters for the GA are: population size equal to 24 individuals, 50 generations over which solution is to evolve, crossover probability 0.85, one point mutation mode with adjustable rate, initial mutation rate 0.005, minimum mutation rate 0.001, maximum mutation rate 0.0185, and full generational replacement reproduction plan with elitism.

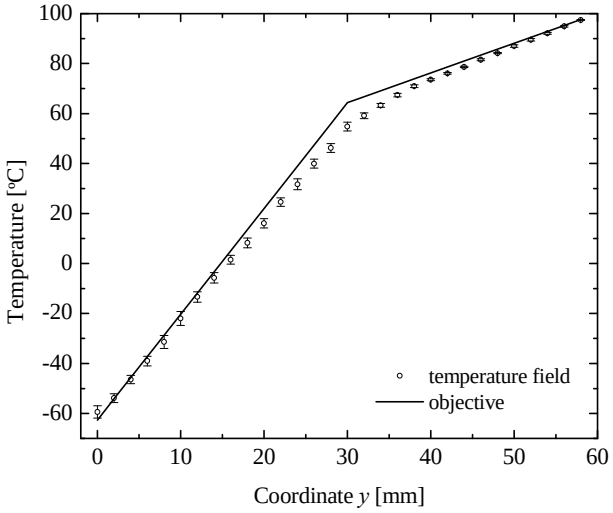

Figure 9: Objective and resultant temperature fields for the first example.

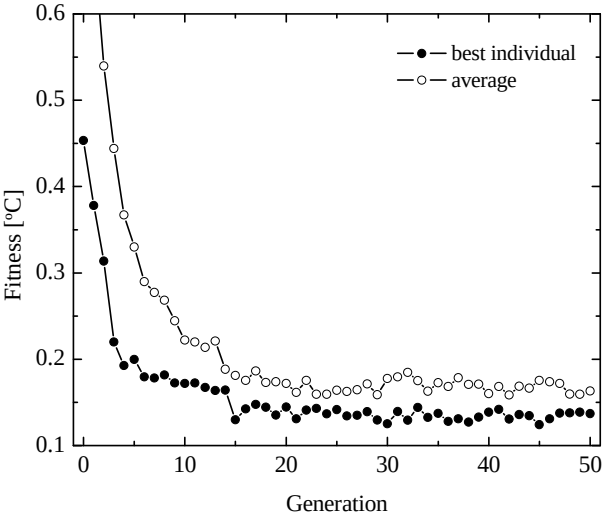

Figure 10: Fitness evolution for the first example: best-of-generation and average results.

Figure 10 illustrates the evolution of the fitness function in terms of the generation number for a typical computer run. Results are plotted for the best individual (the most fitted) in each generation and the average value for all the individuals. A minimum is achieved after approximately 30 generations. It is worth noting that the convergence for the best individual is not monotonous, but there are small occasional increments in the fitness function as the optimization procedure progresses. These increments are a consequence of the random nature of the microstructure. Sample geometries are generated for each generation following the design variables values f_i . But due to the random nature of the microstructure the same set of design values does not produce the same model geometries and consequently the fitness function varies. This means that even for the case when no improvement is made by the GA in a generation and so the best fitted individual is kept, the fitness function value could be reduced or augmented. This phenomenon is reduced by enlarging the RVE size, indicating that the fluctuations in the fitness function evolution are negligible with respect to the characteristic temperature of the example. Note that in the present example the fluctuations in the fitness function can be estimated in approximately 0.01 °C, and they are negligible compared with the overall temperature difference across the sample (162 °C).

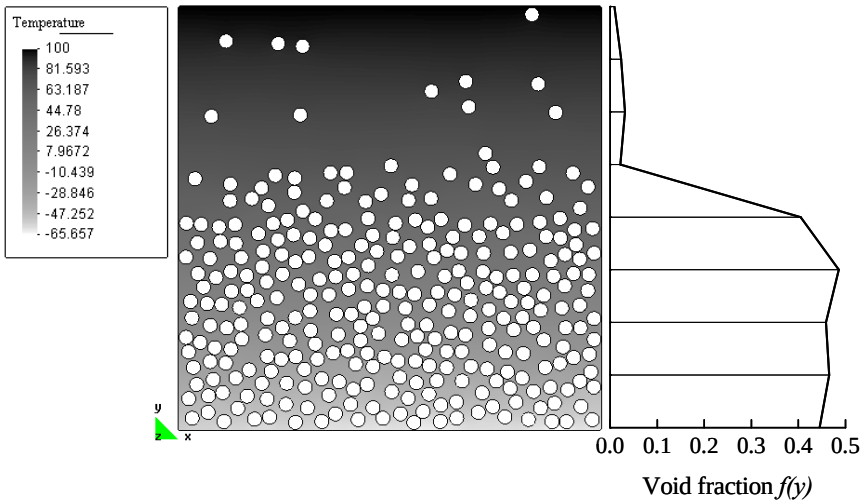

Figure 11: First example: (a) optimized microstructure with temperature-map, and (b) void fraction solution.

The optimized microstructure is shown in Figure 11 together with the contour plot of the temperature field and the optimal void volume fraction (i.e. solution f_i = 0.445, 0.465, 0.458, 0.486, 0.405, 0.022, 0.032, 0.023, 0.009). Besides the final temperature distribution is plotted in Figure 9 with the error bars indicating the dispersion of the results. It can be seen that the maximum difference between the objective function and the optimized result occurs in the neighborhood of $y = L/2 = 30$ mm, the position where the objective function presents an abrupt change in the slope due to the discontinuity in the conductivity. As it was expected the optimization procedure fails to reproduce this transition because it has been designed to produce smooth variations in the void volume fraction.

5.2 Smooth temperature distribution

The second example deals with a more challenging problem. In this case the sample conductivity varies continuously in the y-direction. The variation is chosen to have Gaussian-like shape (see Figure 12) and it is written in terms of Padé polynomials (Jones and Thron, 1980) as follows:

$$\frac{k(y)}{k_0} = k_{\min} + \frac{A}{(y-\mu)^2/\sigma + 2} \tag{5}$$

where the constants were set $k_{\min}$ = 0.2805, $A = 3\sqrt{2}/\pi$, $\mu = L/2 = 30$, $\sigma = 20$. It is worth noting that like in the previous example the maximum and minimum conductivity values correspond to the void volume fractions f=0 and f=0.5 respectively.

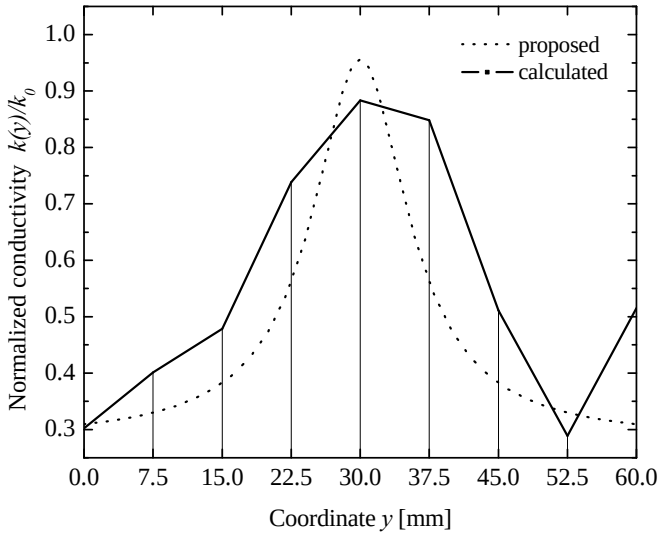

Figure 12: Proposed and obtained conductivity variations along the sample.

The problem boundary conditions are similar to those of the first example but with prescribed temperatures T_1=20°C and T_2=100°C along the sides y=0 mm y=60 mm respectively. The resulting objective temperature field is

$$T(y) = 0.3133 + 1.989 \cdot y - 16.41 \cdot \tan^{-1}\left(0.0857 \cdot y - 2.5690\right). \tag{6}$$

The GA parameters were set equal to that of the first example.

The evolution of the fitness function with the generations is plotted in Figure 13 for 2 computer runs. The behavior of the fitness function is in general similar to that of the first example. The minimum is achieved after approximately 20 generations and there exist small fluctuations due to the random nature of the microstructure.

Figure 14 depicts the microstructure of one of the best fitted individuals together with the contour plot for the temperature field and the optimal void volume fraction (f_i = 0.477, 0.383, 0.319, 0.143, 0.059, 0.079, 0.295, 0.492, 0.292). In accordance with the maximum conductivity values, the minimum void volume fraction occurs in the central part of the sample.

The comparison between the objective function and the resulting temperature field is plotted in Figure 15. The computed solutions are in excellent agreement with the objective function.

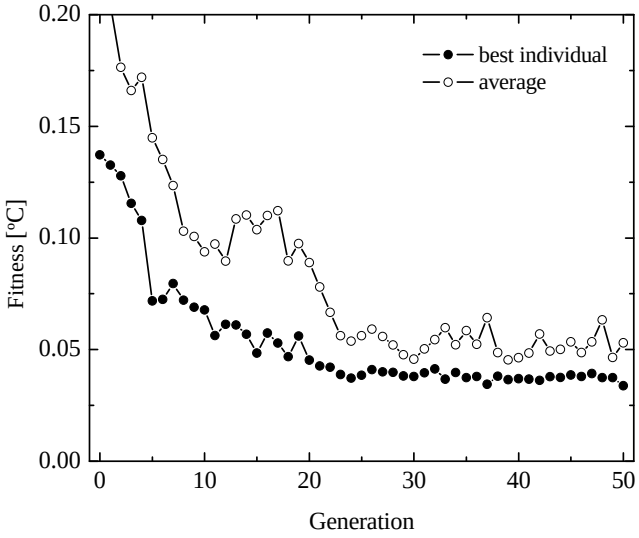

Figure 13: Fitness evolution for the second example: best-of-generation and average results.

Finally, the void volume fraction results in Figure 14b were correlated to the conductivity in equation 5 by means of equation 1. The result is plotted in Figure 12. It can be seen that the resulting conductivity posses the same general trend of that used for the formulation of the problem, with the maximum value in the sample central zone

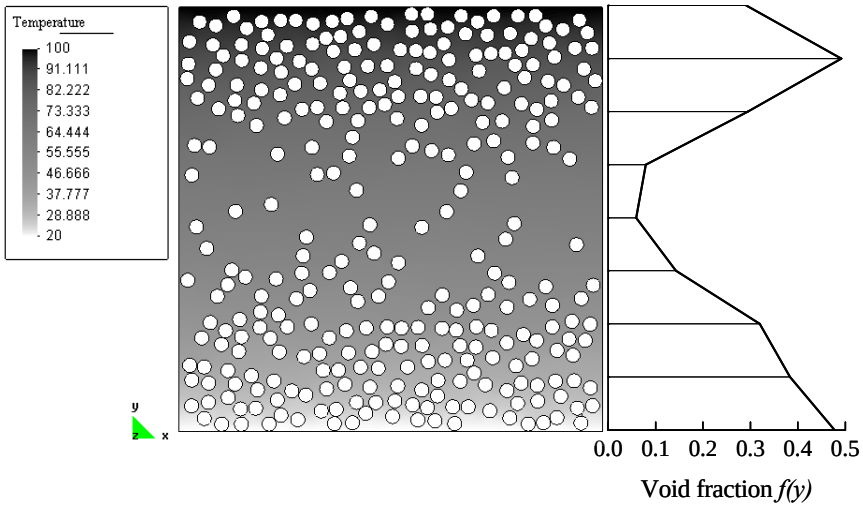

Figure 14: Second example: (a) optimized microstructure with temperature-map, and (b) void fraction solution.

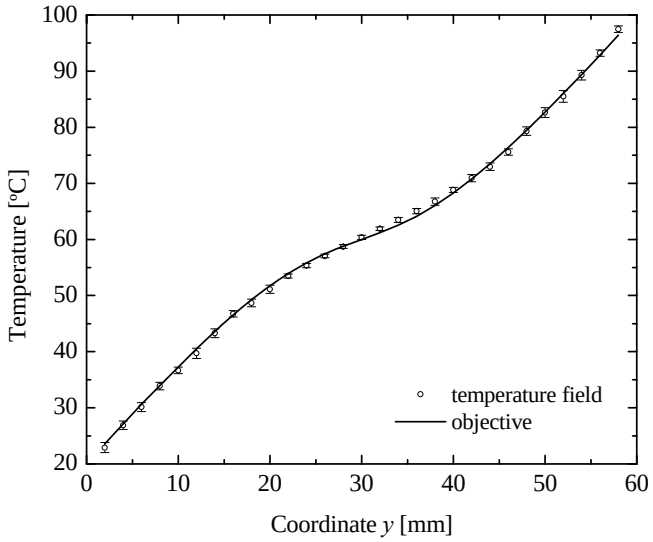

Figure 15: Objective and resultant temperature fields for the second example.

6 CONCLUSIONS

It has been presented in this work an efficient numerical tool for the design of micro-heterogeneous microstructures with functional-graded thermal conductivity. The devised methodology is based on a parallel Genetic Algorithm (GA) as optimization method with a Fast Multipole Boundary Element Method (FMBEM) code for the evaluation of the fitness function using representative volume elements (RVE).

The FMBEM is specially suited for the optimization method: the boundary-only discretization strategy makes the model data generation a simple task, while the fast multipole formulation results in important savings in computing time when compared to direct BEM.

Two validation examples demonstrate the performance of the implementation. The proposed methodology is general and robust and can be easily extended to optimize more complex microstructures with the distribution of inclusions and/or holes, their shapes, orientations and material properties as design variables.

ACKNOWLEDGMENTS

This work has been partially supported by the projects ALFA II ELBENET “Europe Latin America Boundary Element Network” of the European Union, PROSUL 040/2006 “Optimization of microstructures of polymer-matrix composites” (CNPq-Brazil), PICT 12-14114 of the Agencia Nacional de Investigaciones Científicas y Técnologicas of Argentina, and CONICET.

REFERENCES

Aliabadi M.H, and Wrobel L.C. “The Boundary Element Method” John Wiley & Sons, Chichister, UK (2002)

Charbonneau P. and Knapp B. "A User's Guide to PIKAIA 1.0" NCAR Technical Note TN-418+IA (1995)

Charbonneau P. and Knapp B. "PIKAIA: Optimization (maximization) of user-supplied 'fitness' function ff over n-dimensional parameter space x using a basic genetic algorithm method." High Altitude Observatory, National Center for Atmospheric Research, Boulder

CO 80307-3000, US. (http://download.hao.ucar.edu/archive/pikaia)
Goldberg D. E. “Genetic Algorithms in search, optimization & machine learning”, Addison-Wesley, USA (1999)
Jones, William B.; Thron, W. J. Continued Fractions: Theory and Applications. Reading, Massachusetts: Addison-Wesley Publishing Company, 185-197 (1980).
Liu Y. J. and Nishimura N. “The Fast Multipole Boundary Element Method for Potential Problems: A Tutorial”. Engineering Analysis with Boundary Elements, 30, 5, 371-381 (2006)
Press W.H., Teukolsky S.A., Vetterling W.T. and Flannery B.P. “Numerical Recipes in Fortran 77”, Second Edition. Cambridge University Press, Cambridge, UK (1992)
Ruys A. J., Popov E. B., Sun D., Russell J. J. and Murray C. C. J. “Functionally graded electrical/thermal ceramic systems” Journal of the European Ceramic Society, 21, 10-11, 2025-2029 (2001)
Zohdi T.I. and Wriggers P. “Introduction to Computational Micromechanics” Lecture Notes in Applied and Computational Mechanics, Volume 20, Springer-Verlag, Berlin (2005)